

Design of Randomized Space-Time Block Codes for Cooperative Multi-Hop Strip-Shaped Networks



By

Sidra Shaheen Syed

2012-NUST-MS-EE(S)-60907

Supervisor

Dr. Syed Ali Hassan

Department of Electrical Engineering

A thesis submitted in partial fulfillment of the requirements for the degree
of Masters in Electrical Engineering (MS EE-TCN)

In

School of Electrical Engineering and Computer Science,
National University of Sciences and Technology (NUST),

Islamabad, Pakistan.

(March 2015)

Approval

It is certified that the contents and form of the thesis entitled “**Design of Randomized Space-Time Block Codes for Cooperative Multi-Hop Strip-Shaped Networks**” submitted by **Sidra Shaheen Syed** have been found satisfactory for the requirement of the degree.

Advisor: **Dr. Syed Ali Hassan**

Signature: _____

Date: _____

Committee Member 1: **Dr. Adnan Khalid Kiani**

Signature: _____

Date: _____

Committee Member 2: **Dr. Hassaan Khaliq**

Signature: _____

Date: _____

Committee Member 3: **Dr. Rizwan Ahmad**

Signature: _____

Date: _____

Dedication

I dedicate this thesis to my parents, brother, teachers, and friends who have been supportive throughout my research phase.

Certificate of Originality

I hereby declare that this submission is my own work and to the best of my knowledge it contains no materials previously published or written by another person, nor material which to a substantial extent has been accepted for the award of any degree or diploma at NUST SEECS or at any other educational institute, except where due acknowledgement has been made in the thesis. Any contribution made to the research by others, with whom I have worked at NUST SEECS or elsewhere, is explicitly acknowledged in the thesis.

I also declare that the intellectual content of this thesis is the product of my own work, except for the assistance from others in the project's design and conception or in style, presentation and linguistics which has been acknowledged.

Author Name: Sidra Shaheen Syed

Signature: _____

Acknowledgment

I am thankful to Almighty Allah, most Gracious, who in His infinite mercy has guided me and enlightened my mind to complete this work. I am highly indebted to my parents for their continuous support that made every opportunity available to me throughout my life.

My very special thanks to my promoter Dr. Syed Ali Hassan, who gave me the opportunity to work under his supervision in his research group. The experience I have had with Dr. Syed Ali Hassan over the past two years cannot be summed up in a hackneyed phrase or saying, but I would like to express my gratitude and appreciate him for guiding me during the course of my research work with his unique style and sympathetic attitude.

I would like to thank my committee members, Dr. Adnan Khalid Kiani, Dr. Hassan Khaliq, and Dr. Rizwan Ahmad for reviewing and evaluating my thesis.

My special thanks to Dr. Sajid Ali for his friendly assistance, insightful discussions and guidance. His recommendations have introduced me with advance concepts and techniques of linear algebra and directional statistics.

Thanks to all those friends and teachers who contributed towards the successful completion of my dissertation.

Sidra Shaheen Syed

Abstract

Space-time block code (STBC) is one of the most important techniques for designing orthogonal channels thereby adding diversity in wireless cooperative multi-hop networks. These STBCs are used by the decode-and-forward (DF) nodes at each hop of the cooperative strip-shaped networks. To deal with the uncertainty of DF nodes in opportunistic strip-shaped cooperative network, partially randomized and near-orthogonal random space-time block codes (STBCs) are designed resulting in orthogonal and near-orthogonal channels respectively. These channels transmit information independently in a fully opportunistic wireless network thereby adding diversity and coding gains. The network is considered to have fixed hop boundaries having constant node density opportunistic large array (OLA), and operating on decode-and-forward (DF) relaying mode. Two types of system models are considered, out of which partially randomized STBC is designed for the one having deterministic node geometry and near-orthogonal random STBC is designed for the one with a completely random node geometry. In order to deal with random number of decode-and-forward nodes, M , in each hop, directional statistical concepts are utilized for the randomization of underlying deterministic STBC letting each node to transmit linear combination of symbols or STBC columns. The transmissions are modeled stochastically using Markov chain.

Network performance is evaluated on the basis of one-hop success probability and coverage for different node geometries, number of nodes per hop, N , and dimensions of STBCs.

Table of Contents

1	Introduction	1
1.1	Opportunistic Large Array Networks	2
1.2	Diversity	3
1.2.1	Diversity Techniques	3
1.3	Introduction to Space-Time Block Codes	4
1.3.1	On the Use of OSTBC for Cooperative Network	5
1.4	Applications of Strip-Shaped OLA Networks	7
1.5	Motivation	7
1.6	Problem Statement	8
1.7	Thesis Organization	8
1.7.1	Chapter 2	8
1.7.2	Chapter 3	8
1.7.3	Chapter 4	9
1.7.4	Chapter 5	9
2	Literature Review	10
3	Partially Randomized Space-Time Block Code	14
3.1	Introduction	14

<i>TABLE OF CONTENTS</i>	viii
3.2 Network Model	15
3.2.1 2D Co-Located Groups Topology	18
3.3 Transmission Modeling	20
3.3.1 Transition Probability Matrix	21
3.3.1.1 Transition Probability Matrix for 2D Grid Strip Network Topology	22
3.3.1.2 Transition Probability Matrix for 2D Co-Located Groups Topology	23
3.4 Results and Analysis	23
4 Near-Orthogonal Space-Time Block Codes	31
4.1 Introduction	31
4.2 Network Description	31
4.3 Near- Orthogonal Random Matrix	34
4.4 Transmission Modeling	36
4.4.1 Markov Chain Modeling of Random Strip OLA Net- work	37
4.5 Results and Analysis	39
5 Conclusion and Future Work	46
5.1 Conclusion	46
5.2 Future Work	47

List of Figures

1.1	Two-hop cooperative network	6
3.1	2D grid strip network layout	15
3.2	2D Co-located groups topology	19
3.3	One-hop success probability for 2D distributed grid network .	25
3.4	Comparison of ρ_{dis} obtained through simulations and analytical model	26
3.5	SNR margin vs. maximum coverage for $M = 6$	27
3.6	SNR margin vs. maximum coverage for various values of M .	28
3.7	One-hop success probability differences between co-located and distributed topologies	30
4.1	Fixed boundary strip network layout with $N = 3$	32
4.2	One-hop success probability comparison between Nearly-orthogonal randomized STBC and antenna selection technique for $L = N = 2$	39
4.3	One-hop success probability for cooperative multi-hop strip-shaped networks for $L = N$	41

4.4	One-hop success probability comparison of near-orthogonal randomized STBC for $L = 2$	42
4.5	Coverage vs. SNR margin for near-orthogonal randomized STBC, $L = N$	43
4.6	Coverage comparison for $L = 2$	44

List of Tables

3.1	Comparison for optimal STBC and node geometry	29
4.1	Comparison for the optimal combination of L and N for $W = 6$	45

List of Abbreviations

Abbreviation	Description
STBC	Space-Time Block Code
OSTBC	Orthogonal Space-Time Block Code
DF	Decode-and-Forward
AF	Amplify-and-Forward
OLA	Opportunistic Large Array
MIMO	Multi-Input Multi-Output
SNR	Signal-to-Noise Ratio
CN	Cooperative Networks

Chapter 1

Introduction

Wireless channels are prone to fading, shadowing, interference, and other types of transmission impairments thus limiting the performance of wireless networks. Whereas these channel fading effects can be highly reduced by exploiting spatial diversity [1].

In wireless ad-hoc sensor networks, each spatially distributed autonomous sensor node acts as a distributed multiple-input multiple-output (MIMO) antenna thereby adding higher diversity gains [2]. Multi-hopping along with added diversity gains and low transmit power (because of point-to-point links between nodes from source to destination) make these networks a best choice for long-range and low power transmissions [3]. In order to add diversity gains for improved link reliability and coverage range, distributed nodes cooperatively transmits the same information towards the intermediate nodes that relays it towards the destination via multi-hopping. This type of transmission is known as cooperative transmissions (CT) and the networks that implements CT are known as cooperative networks (CN). Majorly CN undergoes two types of relaying and these are:

1. *Amplify-and-Forward (AF)*: In this type of relaying technique, the intermediate nodes amplify the source signal received from the previous hop without looking into the content of a message, i.e., no demodulation and decoding takes place at the intermediate relaying nodes [4]. The disadvantage of this relaying technique is that the additive noise will have higher power because of noise amplification along with signal amplification.
2. *Decode-and-Forward (DF)*: In this type of relaying technique, each intermediate node decodes and recovers the symbols transmitted by the source, and if it successfully decodes the source information only then it will be eligible to relay that information to the nodes in its vicinity otherwise, it will not [5]. The difference from AF is that, not all the relays take part in cooperative transmission and the additive Gaussian noise will have low power.

1.1 Opportunistic Large Array Networks

Cooperative network that undergo control flooding at physical layer (PHY) is known as opportunistic large array (OLA) network [6]. Opportunistic large array (OLA) is a transmission phenomenon for achieving cooperative diversity, thereby improving reliability [7], link quality, coverage[8], and energy efficiency[9]. The OLA transmission mode of cooperative communications (CC) is the one in which large groups of low power sensor nodes relay the same message to a far off destination node. This type of network employs decode-and-forward (DF) relaying mode, on the basis of which multi-hop

communication takes place from the source to the destination[6]. The relaying nodes in each hop transmit the same message block towards the nodes in the next hop without any inter-node coordination, i.e., each node is considered to be completely autonomous. Hence, OLA provides a low overhead and low power solution for large dense wireless sensor networks.

1.2 Diversity

One major transmission impairment in wireless communications is multi-path fading because of which signal fades, i.e., the fluctuation in signal strength such that the power of received signal falls below a certain level which results in high bit error rate (BER). Diversity is a technique through which we can combat fading by transmitting replicas of a signal over time, frequency, and space [1]. Hence, diversity can be characterized by number of independent fading paths between a transmitter and a receiver.

1.2.1 Diversity Techniques

There are three techniques by which diversity can be added to wireless networks.

- *Temporal diversity*: In this type, copies of a signal are transmitted over time followed by channel coding and time interleaving. This type becomes practical for the cases where the channel coherence time is small as compared to symbol or signal duration thus, assuring that at different times channel behaves independently.
- *Frequency diversity*: Replicas of a signal is transmitted over frequency

in this diversity type. It becomes applicable when we have small channel coherence bandwidth as compared to signal bandwidth.

- *Spatial diversity*: Also known as antenna diversity is a diversity technique in which copies of a signal are transmitted through different spatially separated antennas. Antennas are considered to have minimum separation in between so that information undergoes independent channel fades. This is an effective diversity technique for combating multipath fading.

Each of these diversity techniques have their own pros and cons such that:

1. Temporal diversity adds diversity at the cost of transmission delay in the network.
2. Frequency diversity adds diversity at the cost of high bandwidth.
3. Spatial diversity adds diversity at the cost of reduced expected data rate.

In order to achieve full diversity at reduced incurring cost, the two diversity techniques temporal and spatial are combined and thus given the name space-time block codes (STBCs). STBCs are explained briefly in next section along with their application to cooperative network.

1.3 Introduction to Space-Time Block Codes

Space-time block coding is a transmit diversity technique that was introduced for MIMO networks in order to add full diversity by the design of orthogonal

channels [10]. The fully orthogonal STBCs (OSTBCs) ensure full diversity. These codes can be represented in a matrix form as

$$\begin{bmatrix} s_1 & s_2 \\ -s_2^* & s_1^* \end{bmatrix},$$

which is the first OSTBC proposed by Alamouti in [10] for collocated MIMO systems. Here, s_1 and s_2 are the two modulated symbols. The rows in the code represents the time slots that will be consumed for a transmission of a symbol block and the columns represents the symbols transmitted from one antenna in their respective time slots. This implies that information is being transmitted over time and space both.

The orthogonality of the code can be revealed by the inner product of the columns, which is zero for the above mentioned case such that

$$s_1 s_2^* - s_2^* s_1 = 0.$$

This is the only proposed OSTBC that ensures full diversity at full rate. All other OSTBCs principled at Alamouti's code either made a compromise between diversity (orthogonality of a code) or rate [11]-[14].

1.3.1 On the Use of OSTBC for Cooperative Network

Although the number and identity of transmitting nodes in CN are not known a priori but, we try to explain how OSTBCs proposed for MIMOs can be used for cooperative network having known number of DF nodes as shown in Fig. 1.1. In Fig. 1.1, a two-hop network having a source, S_o , and destination, D_e , with two intermediate relays R_1 and R_2 respectively are shown.

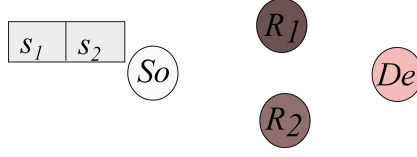


Figure 1.1: Two-hop cooperative network.

In first phase of transmission the source transmits a block of symbols $\begin{bmatrix} s_1 & s_2 \end{bmatrix}$ towards the relays as mentioned in [15, Ch. 6]. Let, the post detection signal-to-noise ratio (SNR) at the two relays is greater than the predefined threshold, τ , defined for the received power. Now these two DF relays cooperatively transmits the message block towards the destination in the next transmission phase on orthogonal channels using Alamouti OSTBC. The received signals during the two time slots at the destination can be represented as

$$\begin{aligned} r_1 &= s_1 h_1 + s_2 h_2 + z_1, \\ r_2 &= -s_2^* h_1 + s_1^* h_2 + z_2, \end{aligned} \quad (1.1)$$

where r_1 and r_2 are the received signals during the two time slots receptively, h_i is the channel gain from the i^{th} relay to the destination, and z_i 's are the additive Guassian noise samples. Receivers having perfect channel-state-information (CSI) combines the received signals as

$$\begin{aligned} \tilde{s}_1 &= h_1^* r_1 + h_2 r_2^* = (|h_1|^2 + |h_2|^2) s_1, \\ \tilde{s}_2 &= h_2^* r_1 - h_1 r_2^* = (|h_1|^2 + |h_2|^2) s_2. \end{aligned} \quad (1.2)$$

These above received symbols \tilde{s}_i received with a diversity gains will then be sent to maximum-likelihood (ML) detector for detecting and decoding of the source symbols.

1.4 Applications of Strip-Shaped OLA Networks

Cooperative multi-hop or OLA strip-shaped networks find its applications in many fields, few of them are given below:

- Smart grid communications [16].
- Battle field surveillance.
- Forrest fire detection.
- Remote Patient monitoring in adjacent rooms and floors .

1.5 Motivation

This thesis targets to design orthogonal and near-orthogonal channels for two nodes geometries of a strip-shaped cooperative multi-hop network in order to combat multi-path fading. This task can be accomplished by using deterministic OSTBCs and then

- Partially randomizing them for strip-shaped OLA network having deterministic two-dimensional (2D) grid geometry with node tagging, resulting in fully-orthogonal STBCs or channels.
- Completely randomizing them for strip-shaped OLA network having random node geometry, resulting in near-orthogonal STBCs and channels.

1.6 Problem Statement

1. To design full orthogonal transmission channels for a 2D grid strip-shaped cooperative multi-hop network.
2. To design near-orthogonal transmission channels for fully opportunistic strip-shaped cooperative multi-hop network having random node geometry.

1.7 Thesis Organization

The rest of the thesis is organized as follows:-

1.7.1 Chapter 2

In chapter 2, background study and some of the related works published in the domain of cooperative multi-hop networks and space-time block codes have been discussed in detail.

1.7.2 Chapter 3

In chapter 3, the design of partially randomized space-time block codes for 2D grid strip-shaped cooperative multi-hop network considering node tagging has been proposed. One-hop success probability and transition probability expressions are derived for the given system model. Results are being analyzed for different deterministic node geometries.

1.7.3 Chapter 4

Chapter 4 discusses the network model for the fully opportunistic OLA network considering random node geometry and fixed hypothetical boundaries between adjacent hops thus, making a multi-hop cooperative network. The design of near-orthogonal randomized STBC has been proposed for this type of network with the help directional statistical concepts. Network performance in terms of success probability and maximum coverage has been evaluated for optimal node density and STBC.

1.7.4 Chapter 5

Chapter 5 finally concludes this thesis and provides some insights to the possible extensions that can be made on this work.

Chapter 2

Literature Review

The real-time multimedia and other web-related services demands high throughput which the next generation networks are aiming to achieve. However, different transmission impairments and channel fading limits the transmission capabilities of a wireless channel including maximum achievable throughput. In this regard, different diversity techniques were proposed as mentioned in chapter 1. But, the one that offers maximum diversity gain for minimum required latency and bandwidth is spatial diversity. Multiple-input multiple-output (MIMO) systems firstly incorporated the spatial diversity technique by using multiple antennas at the transmitter and receiver sides [17]. MIMO systems are the ones that ensure higher throughput values by combating channel fading and transmission impairments. However, this technique becomes impractical for sensor networks because of high antenna installation costs and small sensor size [18].

Laneman in [19] proposed a technique named distributed MIMO in oppose to co-located MIMO for sensor networks in which the spatially distributed sensor nodes acts as virtual MIMO antennas forming an antenna array. The

communication that these types of cooperative networks (CN) undergo is known as cooperative communications resulting in cooperative diversity at the receiving nodes. In [6], authors considered a controlled flooding phenomenon for cooperative communications and proposed a special type of CN known as opportunistic large array (OLA) network. OLA is basically the transmission phenomenon in which the group of nodes transmits the same information on orthogonal fading channels towards the next group of nodes thereby making multiple levels in a network.

In past few years, extensive research has been performed on the modeling of cooperative multi-hop networks and especially OLA networks under different fading [20]-[25], shadowing [3], and interfering environments [26]. Performance analysis under imperfect timing synchronization at the transmitter and receiver side has been studied in [27]. In [28], maximum coverage has been obtained for optimal node deployment, i.e., by arranging the nodes in the form of clusters in one-dimensional (1D) cooperative multi-hop networks. However, all of these works require the message block to be transmitted by the DF nodes on independently fading orthogonal channels after achieving transmit time synchronization. These orthogonal channels must be designed in order to achieve maximum diversity and minimum interference.

Orthogonal space-time block codes (OSTBCs) is a well known diversity technique that helps in transmitting the information on orthogonal channels operating on same frequency band. OSTBCs were firstly designed for the multiple-input multiple-output (MIMO) systems for deterministic number of transmit/receive antennas for achieving lower error probability [10]. On the other hand, in OLA networks the number of DF nodes in each hop is

a random entity. For this many authors have proposed randomized STBCs for distributed cooperative networks (CN). Although an extensive material is available for STBCs of general MIMO systems, very few literature is available on the design of randomized STBCs. In [29], authors have assumed the assignment of orthogonal STBC columns to the decoding nodes by a central entity, which results in extra communication overhead. However, this centralized assignment has been ruled out by making the selection purely local at the node in [30], where each node randomly selects an STBC column with the help of canonical basis vectors given the uniform distribution of these basis vectors. This equi-probable basis will result in diversity loss and hence increased error probability. In [31], randomized STBC designs have been proposed for CN by the introduction of random vectors generated independently at each DF relaying nodes. These random vectors that combine to form a randomized matrix were resulted through different stochastic and directional statistical techniques. Out of all the proposed designs for random vectors the one that out performed in average error probability analysis was the vectors generated uniformly on the surface of unit hypersphere [32]. The reason behind minimum error probability for this randomization technique was that the random independent vectors tends to be nearly orthogonal. Therefore, the product of an orthogonal STBC matrix with a nearly or almost orthogonal vector results in the nearly orthogonal matrix. Hence, this near orthogonality results in minimum interference and thus low average error probability.

All of the above mentioned randomized STBC techniques considered the single source destination pair and the intermediate relays, i.e., a two hop

network. The design of randomized OSTBC (ROSTBC) for multi-hop CN has only been addressed in [33] but the authors have considered amplify-and-forward (AF) relaying with fixed number of nodes in each hop. Therefore in this thesis, we have proposed partially randomized STBC for 2D grid strip OLA network where the DF nodes in each hop were considered random and all the nodes were being tagged where each DF node selects a distinct OSTBC column on the basis of the tag assigned to it. We have also considered to design randomized STBC for fully opportunistic strip OLA network geometry in which the nodes are placed randomly using binomial point process (BPP) in a square region. The randomized STBC proposed in [31] has been used and extended to the multi-hop CN presented in [34] hence, proposing a completely randomized near-orthogonal STBC for OLA network. For both the designs, strict boundaries have been considered to group equal number of nodes in each hop. The networks are modeled by considering the flat Rayleigh fading channel with path loss effects. It has also been assumed throughout this work that the receivers have perfect channel state information (CSI). To the best of our knowledge, no one has addressed to design and to analyze the use of randomized STBC for OLA network having deterministic and random node geometries which has been the main motivation behind this work.

Chapter 3

Partially Randomized Space-Time Block Code

3.1 Introduction

In this chapter, the required design of orthogonal channels for the 2D grid strip-shaped OLA network is discussed. This requirement has been fulfilled by the design of partially randomized STBCs considering tagged nodes. The message block from the decode-and-forward (DF) nodes are mapped on to partially randomized STBCs and the transmitted signal undergoes the Rayleigh fading with additive white Gaussian noise (AWGN). Transmit and receive times synchronization has been assumed throughout our study. Closed form expressions for received power, one-hop success probability and transition probabilities have been derived. System performance has been analyzed on the basis of maximum coverage, total delay, and required SNR margin for different node geometries. The performance of distributed 2D grid strip OLA network is compared with co-located group topology in the

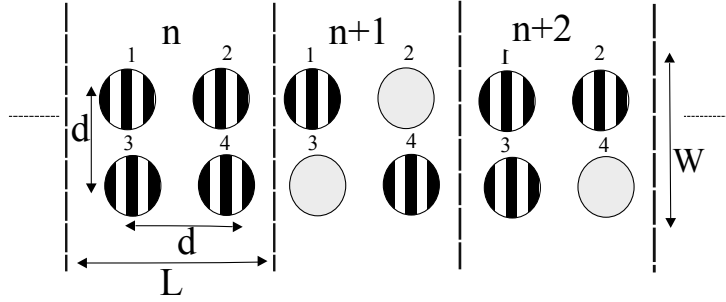


Figure 3.1: 2D grid strip network layout.

end.

3.2 Network Model

In this chapter, we are considering an extended network of nodes that are arranged along a 2D grid, making a 2D strip cooperative network as shown in Fig. 3.1. Each node is a distance d apart from the adjacent nodes along each dimension. For our case, we assume that the nodes, which decode the message in a hop, i.e., the nodes represented by filled circles in Fig. 3.1, relay it synchronously to the nodes in the next hop using an orthogonal space-time block code. In each hop of the 2D strip network, the receiving nodes decode the message on the basis of a modulation dependent threshold. The comparison of the received signal-to-noise ratio (SNR) with the threshold is done at the output of the diversity combiner, and if the received SNR is greater than or equal to this threshold, the node will be able to decode the message and vice versa.

For the 2D strip network shown in Fig. 3.1, the nodes are numbered from top to bottom and then from left to right. The length of the level or hop is the number of nodes present along the horizontal direction, while the number

of nodes along the vertical direction represents the width of the hop. The product of length and width gives the total number of nodes present in one hop of the 2D strip network. In general, we have, $M = L \times W$, where the total number of participating nodes in each hop is, M , L is the length, and W is the width of a hop. In case of M number of nodes in each hop, we consider to use the orthogonal STBC for M transmit antennas, i.e., STBC having M orthogonal columns.

Consider a block of symbols $\mathbf{s} = [s_1 \ s_2 \ \dots \ s_b]^T$ to be transmitted cooperatively towards the destination using M nodes of a level, where $[\cdot]^T$ denotes the transpose operation and b is the total number of symbols that makes a message block. The relay nodes in the n^{th} level use orthogonal STBC to cooperatively transmit the information symbols to the next $(n+1)^{\text{th}}$ level nodes on orthogonal channels. The received signals in P time slots on a k^{th} node of level $(n+1)$ can be represented as

$$\mathbf{y}_{(n+1)}^{(k)} = P_t \mathcal{G} (\mathbf{h}^{(k)} \circ I(n)) + \mathbf{z}, \quad (3.1)$$

where $\mathbf{y}_{(n+1)}^{(k)} \in \mathbb{C}^{P \times 1}$, i.e., $\mathbf{y}_{(n+1)}^{(k)} = [y_1^{(k)} \ y_2^{(k)} \ \dots \ y_P^{(k)}]^T$ is the received signal vector at the k^{th} node of the $(n+1)^{\text{th}}$ hop and P_t is the transmitted power, which is assumed equal for each node. The matrix $\mathcal{G} \in \mathbb{C}^{P \times M}$ is the complex orthogonal STBC having P rows and M columns, i.e., STBC for M number of cooperating nodes, and transmission of each message block from one level to the next takes on P time slots. The vector $\mathbf{h}^{(k)} \in \mathbb{C}^{M \times 1}$, i.e., $\mathbf{h}^{(k)} = [h_1^{(k)} \ h_2^{(k)} \ \dots \ h_M^{(k)}]^T$ is the channel vector and the subscript of individual elements denotes the transmitting node from the previous level. The vector $I(n) = [\mathbb{I}_1(n) \ \mathbb{I}_2(n) \ \dots \ \mathbb{I}_M(n)]^T$ is the indicator or state vector for the nodes of the previous n^{th} level and its elements take on binary values indicating the DF nodes of the previous level. For instance, if the

first node of the previous level has decoded the information, then $\mathbb{I}_1(n) = 1$, otherwise $\mathbb{I}_1(n) = 0$. The vector, \mathbf{z} , is the complex Gaussian noise vector and the mathematical operator \circ denotes the Hadamard product between two vectors.

Each $h_j^{(k)}$ from the channel vector represents the fading channel from the j^{th} relay node of the n^{th} hop to the k^{th} receiving node of the $(n+1)^{\text{th}}$ hop. The channels between j^{th} transmitting node from the previous level to one of the node of next level are stacked to form a vector and this vector is represented in (3.1) as, $\mathbf{h}^{(k)}$. Each of these channel gains between a node pair also takes into account the path loss between them. Therefore, we define $h_j^{(k)}$ as, $h_j^{(k)} = \frac{\alpha_{jk}}{d_{jk}^\beta}$, here α_{jk} is the complex Gaussian random variable with zero mean and unit variance representing Rayleigh fading, d_{jk} is the Euclidian distance between the two nodes, and β is the path loss exponent that can be in range of 2-4. The channel is assumed static during the transmission of one block. Therefore, $h_j^{(k)}$ remains constant for the transition of one message block. At each k^{th} receiver, decoding takes place by using the decoding matrix as given in (3.2), i.e.,

$$\tilde{\mathbf{s}}^{(k)} = \mathcal{H} \mathbf{y}_{(n+1)}^{(k)}. \quad (3.2)$$

In (3.2), $\mathcal{H} = \mathcal{G}^H$ is the decoding matrix and is assumed to be known at receiver and $[\cdot]^H$ represents the Hermitian operator. The above equation shows the maximal ratio combining (MRC) at the k^{th} node, Where, $\tilde{\mathbf{s}}^{(k)}$ is the received message block. After substitution of respective matrices, the above expression can be represented as

$$\tilde{\mathbf{s}}^{(k)} = \sum_{j \in \mathbb{N}_n} |h_j^{(k)}|^2 \mathbf{s}. \quad (3.3)$$

This shows that the whole block of symbols will be received with a gain of $|\mathbb{N}_n|$, where $|\mathbb{N}_n|$ is the cardinality of set \mathbb{N}_n , which consists of the indices of the nodes that decoded the signal perfectly at the n^{th} hop. Similarly, the message signal in the form of block will be received at each node of the $(n+1)^{\text{th}}$ level. The decision of the node to decode the message perfectly, as mentioned before, depends upon the transmission threshold, τ , i.e., if the received power at the k^{th} node is greater than or equal to τ , the node will correctly decode the message block. Hence the expression for the received power from (3.3) can be given as

$$Pr_{(n+1)}^{(k)} = P_t \sum_{j \in \mathbb{N}_n} |h_j^{(k)}|^2. \quad (3.4)$$

From (3.4), it can be observed that the received power at a receiving node depends on the transmitted power, distance between the adjacent nodes, path loss exponent, and Rayleigh fading channel gain of the nodes that decoded the message correctly in the previous n^{th} hop. This channel gain from the nodes that have correctly decoded, depends upon the Euclidean distance between the nodes. It has been assumed that all the nodes that correctly decode the message in a hop or level, relay the symbols of a message block to the nodes in the next level at the same time, i.e., there is perfect transmit synchronization between the nodes along with perfect timing recovery at each receiver [22].

3.2.1 2D Co-Located Groups Topology

In this subsection, we consider a different topology in which the nodes in each level are placed closely in a co-located fashion to form a group as shown in

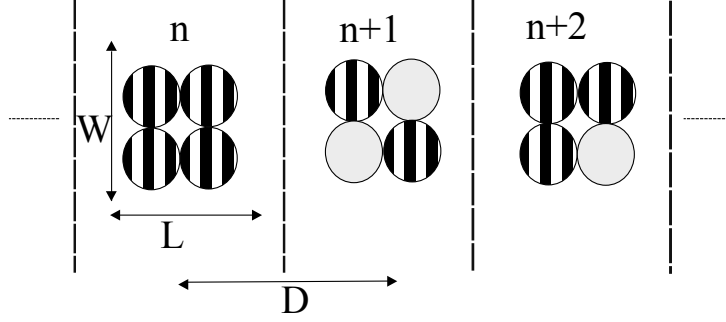


Figure 3.2: 2D Co-located groups topology.

Fig. 3.2. The only difference between the distributed 2D grid strip topology and the 2D co-located topology is the distance between the adjacent nodes, which is quite negligible for the co-located group case. Hence, this negligible spacing between the nodes can therefore be ignored. The only distance that can be taken into consideration is the inter-group distance, and that can be represented as $D \approx Ld$, where L is the number of co-located nodes present along the length in each group and d is the inter node distance in the distributed topology. This means that all nodes of one group are approximately D distance apart from the nodes of the group in the next level. All other assumptions, e.g. synchronization and timing recovery will also remain valid for this model. Similarly, the co-located nodes from each group that decodes the message use orthogonal STBCs to cooperatively transmit the message to the group of nodes in the next level and therefore (1) remains valid for this case also. The only difference as mentioned before is the inter-group distance, D , instead of inter-node distance, d , which in turn effects the path loss and so the channel gain between any two transmitter receiver node pair. i.e., $h_j^{(k)}$ can now be expressed for co-located topology as, $h_j^{(k)} = \frac{\alpha_{jk}}{D^\beta}$.

3.3 Transmission Modeling

As it can be deduced from (3.1) that the decision of the nodes of the present level to decode the message block, only depends upon the nodes that have decoded the message in the previous hop or level only. Therefore, this network behavior can be modeled using Markov chain, where each node in a hop can either be in state 1 or 0 if it has perfectly decoded or not, respectively. Hence, the state of each j^{th} node of n^{th} level or time instant, can be represented by a binary indicator random variable as used in (3.1), i.e, $\mathbb{I}_j(n)$.

Therefore, the state of the network at any time instant n can be represented as M -bit binary word $\tilde{I}(n)$. This indicator RV collectively represents the state of each node of present hop as

$$\tilde{I}(n) = \begin{bmatrix} \mathbb{I}_1(n) & \mathbb{I}_{(W+1)}(n) & \cdots & \mathbb{I}_{(L-1)(W+1)}(n) \\ \mathbb{I}_2(n) & \cdot & & \cdot \\ \cdot & \cdot & \cdot & \cdot \\ \cdot & \cdot & \cdot & \cdot \\ \cdot & \cdot & \cdot & \cdot \\ \mathbb{I}_W(n) & \mathbb{I}_{2W}(n) & \cdots & \mathbb{I}_M(n) \end{bmatrix}. \quad (3.5)$$

For example, from Fig. 3.1, at level $(n+1)$, $\mathbb{I}_1(n+1)=1$, $\mathbb{I}_2(n+1)=0$, $\mathbb{I}_3(n+1)=0$, and $\mathbb{I}_4(n+1)=1$. Therefore, $\tilde{I}(n+1) = \begin{bmatrix} 1 & 0 \\ 0 & 1 \end{bmatrix}$. In order to convert the above state representation into linear or M -tuples form, i.e., $I = [\mathbb{I}_1 \ \mathbb{I}_2 \ \cdots \ \mathbb{I}_M]^T$, *vec* vector operation is applied to (3.5) as $I(n) = \left\{ \text{vec} \left[\tilde{I}(n) \right] \right\}^T$. Hence, state of the network in Fig. 3.1 at time instant $n+1$ can be expressed as $I(n+1) = [1001]^T$. At this point 2D Markov chain has taken the form of 1D representation. The state space will have 2^M-1 transient states in addition to an absorbing state that eventually terminates

the transmission. An absorbing state is the state in which all the nodes of a hop fail to decode the message block, thus terminating the message propagation.

3.3.1 Transition Probability Matrix

The Markov chain, $I(n)$ can be defined completely by union of two sets, the transient state space X , i.e., $X = \{1, 2, \dots, 2^{M-1}\}$ and $\{0\}$ the absorbing state. Each element of the set X will take on a binary word representation form, which can be termed as indicator or state vector. The other set $\{0\}$ is the set of all zeros and there is always a non-zero probability of transiting to this state which increases asymptotically as, $\lim_{n \rightarrow \infty} \mathbb{P}\{I(n) = 0\} \nearrow 1$.

The concept of absorption with non-zero positive probability results in the quasi-stationary distribution for the given Markov chain [22]. An irreducible and right sub-stochastic transition probability matrix \mathbf{P} having dimensions $(2^M - 1) \times (2^M - 1)$ is then formed by removing the transitions to or from the absorbing state. The Perron-Frobenius theorem is then invoked on \mathbf{P} to get the maximum eigenvalue and the left eigenvector.

Each entry of the transition probability matrix represents the probability of being transiting to one of each possible transient states. Whereas, each state tuple depends upon the binary state of each node at any specific level or time instant say n , i.e., the decoding probability of k^{th} node in n^{th} level can be given as $\mathbb{P}\{\mathbb{I}^{(k)}(n) = 1\} = \mathbb{P}\{\text{Pr}^{(k)}(n) \geq \tau\}$. Whereas, $1 - \mathbb{P}\{\text{Pr}^{(k)}(n) \geq \tau\}$ or $\mathbb{I} = 0$ is the probability of being in outage, and $\mathbb{P}\{Pr^{(k)}(n) \geq \tau\}$ can be written as $\mathbb{P}\{Pr^{(k)}(n) \geq \tau\} = \int_0^\infty f_{pr^{(k)}}(y) dy$. In this expression $f_{pr^{(k)}}(y)$ is the probability density function (PDF) of received power at node k . The

distribution of received power Pr depends upon the topology in which the nodes are arranged, i.e, the PDF of received power at a node may follow different distributions in case of distributed and co-located topologies.

3.3.1.1 Transition Probability Matrix for 2D Grid Strip Network Topology

For distributed 2D grid strip topology, the received power at the k^{th} node is the sum of the the exponentially distributed powers from the previous level with distinct parameter $\lambda_j^{(k)}$. These powers are exponentially distributed because of the square of each channel gain as in (3.3), and the sum of these $|\mathbb{N}_n|$ exponentially distributed powers results in a hypoexponential distribution [22], that can be given as, $f_{pr}^{(k)}(y) = \sum_{j=1}^{\mathbb{N}_n} C_j^{(k)} \lambda_j^{(k)} \exp(-\lambda_j^{(k)} y)$. Hence, one-step probability of transiting from state a to state b will be,

$$\mathbb{P}_{ab} = \prod_{k \in \mathbb{N}_{n+1}^{(b)}} \left\{ \sum_{j \in \mathbb{N}_n^{(a)}} C_j^{(k)} \exp(-\lambda_j^{(k)} \tau) \right\} \prod_{k \in \bar{\mathbb{N}}_{n+1}^{(b)}} \left\{ 1 - \sum_{j \in \mathbb{N}_n^{(a)}} C_j^{(k)} \exp(-\lambda_j^{(k)} \tau) \right\}. \quad (3.6)$$

where $\sum C_j^{(k)} \exp(-\lambda_j^{(k)} \tau)$ is the probability of success at node k , $\lambda_j^{(k)} = \frac{(d_{jk})^\beta \sigma_j^2}{Pt}$, and $C_j^{(k)} = \prod_{\varsigma \neq j} \frac{\lambda_\varsigma^{(k)}}{\lambda_\varsigma^{(k)} - \lambda_j^{(k)}}$. The sets $\mathbb{N}_{n+1}^{(b)}$ and $\bar{\mathbb{N}}_{n+1}^{(b)}$ represents the indices of DF nodes and unsuccessful nodes (nodes having $\mathbb{I}^{(k)}(n) = 0$) of state b at the $(n+1)^{th}$ level, respectively.

3.3.1.2 Transition Probability Matrix for 2D Co-Located Groups Topology

Similarly in this case, the received power at each node in group again will be the sum of exponentially distributed powers from the DF nodes of the previous nodes but with same parameter $\tilde{\lambda} = \frac{D^\beta \sigma_k^2}{P_t}$. As the inter-node distance is almost negligible and the nodes in a level are co-located to form a group therefore, they will have the same path losses, and distribution parameter to the nodes in the next level. Hence, the exponentials having same parameter will result in a Gamma distribution for the received power [35], and the received power PDF will be,

$$f_{pr}^{(k)}(y) = \frac{1}{(|\mathbb{N}_n| - 1)!} \tilde{\lambda}^{|\mathbb{N}_n|} y^{(|\mathbb{N}_n| - 1)} \exp(-\tilde{\lambda}y). \quad (3.7)$$

Hence, the one step success probability at k^{th} node of the next level is, $\exp(-\tilde{\lambda}\tau) \sum_{j=0}^{|\mathbb{N}_n^{(a)}| - 1} \frac{(\tilde{\lambda}\tau)^j}{j!}$. The one step success probability in (3.6) will be replaced by this expression for the co-located groups case, and the final expression then comes out to be,

$$\mathbb{P}_{ab} = \prod_{k \in \mathbb{N}_{n+1}^{(b)}} \left\{ \exp(-\tilde{\lambda}\tau) \sum_{j=0}^{|\mathbb{N}_n^{(a)}| - 1} \frac{(\tilde{\lambda}\tau)^j}{j!} \right\} \prod_{k \in \bar{\mathbb{N}}_{n+1}^{(b)}} \left\{ 1 - \exp(-\tilde{\lambda}\tau) \sum_{j=0}^{|\mathbb{N}_n^{(a)}| - 1} \frac{(\tilde{\lambda}\tau)^j}{j!} \right\}. \quad (3.8)$$

3.4 Results and Analysis

In this section, we present the results that demonstrate the system performance by the implementation of different STBCs for different number of nodes, M , in each level, followed by some comparisons and analysis. We

first present the relative comparison of one-hop success probability obtained analytically through Perron-Frobenius eigenvalue, ρ , of the transition matrix in (3.6) for $M = 6$, but with the variation in the values of L and W for distributed case. This one-step success probability, ρ_{dis} , for distributed case is shown as function of SNR margin, γ , where γ is the normalized SNR with respect to τ , which can be defined as $\gamma = \frac{P_t}{\sigma^2\tau}$. The values for some other system parameters are $d = 1$, $\beta = 2$ or 3 , and $P_t = 1W$.

Fig. 3.3 demonstrates the behavior of one-hop success probability, ρ_{dis} , for the distributed network topology for $\beta = 2$. Hop size M is kept constant for this case, i.e., $M = 6$, and different combinations of L and W are considered. To carry out this comparison, we used orthogonal STBC for six antennas given in [11] and it takes on 30 time slots to transmit a block of 18 symbols cooperatively from one hop to the next. Generally, it can be observed that for all possible combinations of L and W , one-hop success probability increases with the increase in γ , where increase in γ results in decrease of τ , making more nodes to correctly decode the information. However, for a specific value of γ , the first two 2D distributed cases seem to achieve better ρ_{dis} as compared to 1D distributed case, i.e., $L = 6$ and $W = 1$. For the 2D case, the one combination having greater number of nodes across the width, ($L = 2, W = 3$) provides better ρ_{dis} as compared to the other combination in which there are more nodes across the length of a hop ($L = 3, W = 2$). The reason behind this behaviour is the Euclidean distances between the nodes of two hops that are least for the first case, on average, as compared to the other two cases. This distance in turn effects the path loss and hence the performance gain.

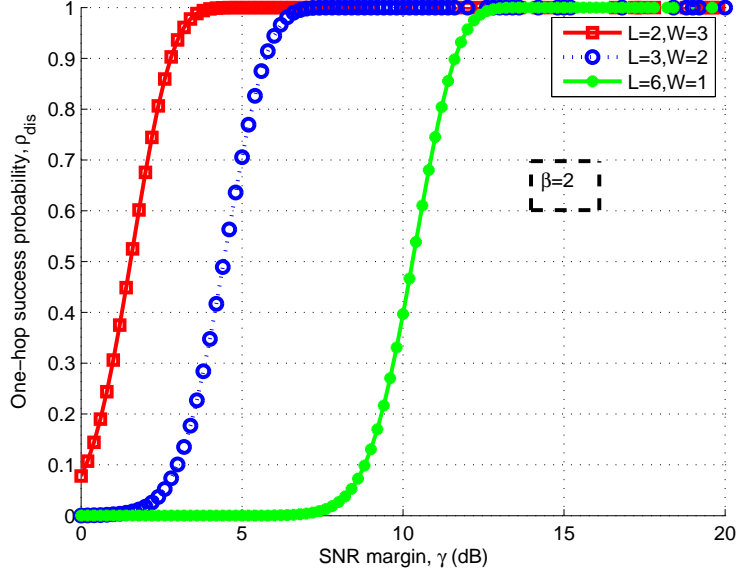


Figure 3.3: One-hop success probability for 2D distributed grid network.

Fig. 3.4 represents the difference between the one-hop success probability, ρ_{dis} , obtained from simulations and from analytical model. The value of parameter M used in Fig. 3.4 are $M = 4$ ($L = 2$, $W = 2$) and $M = 6$ ($L = 3$, $W = 2$) for different values of γ . The plot shows that the analysis and simulation results match closely for different cases. In simulations, the one-hop success indicates that at least one node decodes the message correctly. The forthcoming results are all based on theoretical models.

In Fig. 3.5, the network performance is analyzed by evaluating the coverage in terms of maximum number of hops traversed or the maximum number of nodes along the length of network that receives the information with a given quality of service (QoS) constraint, η . In our case, we obtain the maximum coverage when we require our system to operate at above 90% success probability for all hops, i.e., $\eta \geq 0.9$. Now if ρ_{dis} is the one-hop success prob-

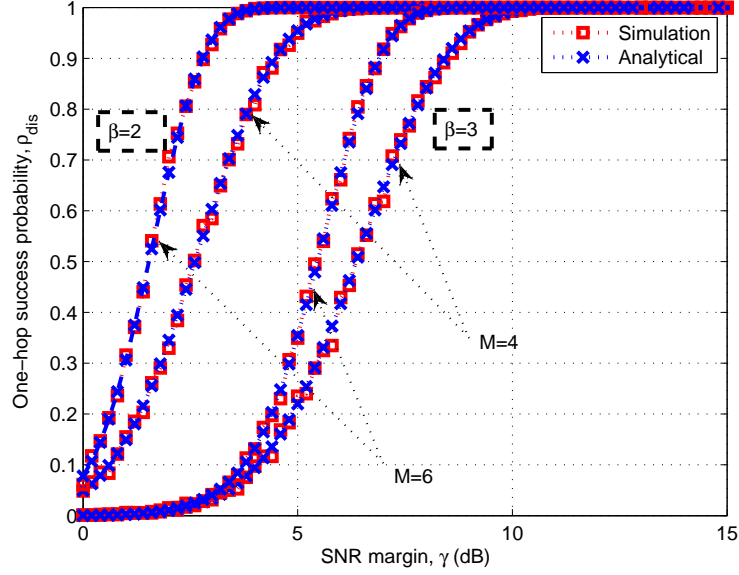


Figure 3.4: Comparison of ρ_{dis} obtained through simulations and analytical model.

ability then the success probability until ℓ^{th} hop will be ρ_{dis}^ℓ . Therefore, to transmit the information block to ℓ^{th} hop with 90% success probability, we require, $\rho_{dis}^\ell \geq \eta$. From here it can be deduced that the maximum number of hops that can be traversed by the information blocks on average, with the required success probability are $\ell \leq \frac{\ln \eta}{\ln \rho_{dis}}$. This maximum hop value, ℓ when multiplied with the L results in the average number of nodes, \mathcal{C} , that receives the information. The plot is generated for the three mentioned geometries for $M = 6$, and it can be seen from Fig. 3.5 that the combination $L = 2$ and $W = 3$ provides the highest coverage value at each possible SNR margin as compared to the other two combinations of L and W .

Fig. 3.6 shows the general effect of increasing hop size M on the coverage for various values of W , and for a fixed L . This figure shows that while

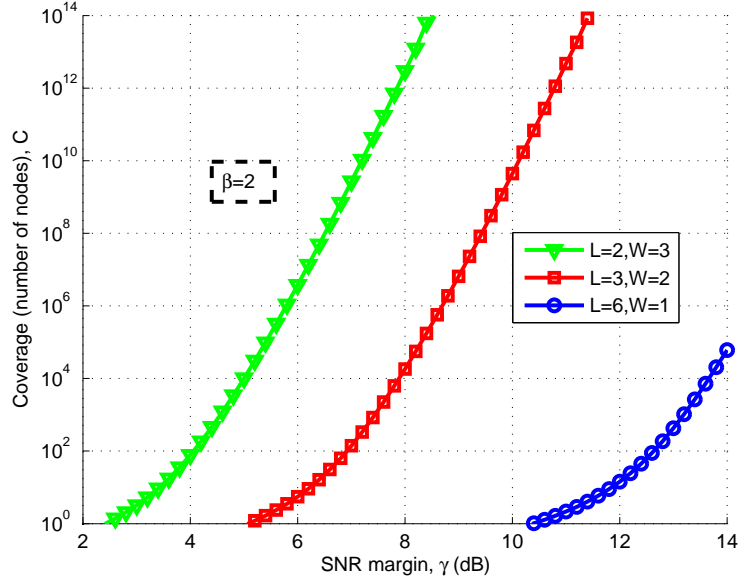


Figure 3.5: SNR margin vs. maximum coverage for $M = 6$.

considering a certain geometry of nodes, the increase in M results in higher coverage for the same required SNR margin.

The overall comparison of the distributed 2D strip network topology is being summarized in Table 3.1, where P is the number of time slots that an STBC takes on, T_d is the overall delay, and R is the rate. The table quantifies the effect on various parameters for a fixed coverage range, i.e., $\mathcal{C} = 24$, where nodes can be arranged in different geometries. For the case in which $M = 6$, $L = 2$, and $W = 3$, we use an STBC of $3/5$ rate provided in [11] that transmits a block of 18 symbols from one hop to the next in 30 time slots. Therefore, the transmission of a message block to the 24^{th} node or 12^{th} hop, takes on 360 time slots. Thus, $3/5$ rate STBC transmits the message blocks to 24^{th} node with a maximum rate of $18 \text{ symbols} / 360P$. From Table 3.1, it can be inferred that if the horizontal stretch of a hop contains more

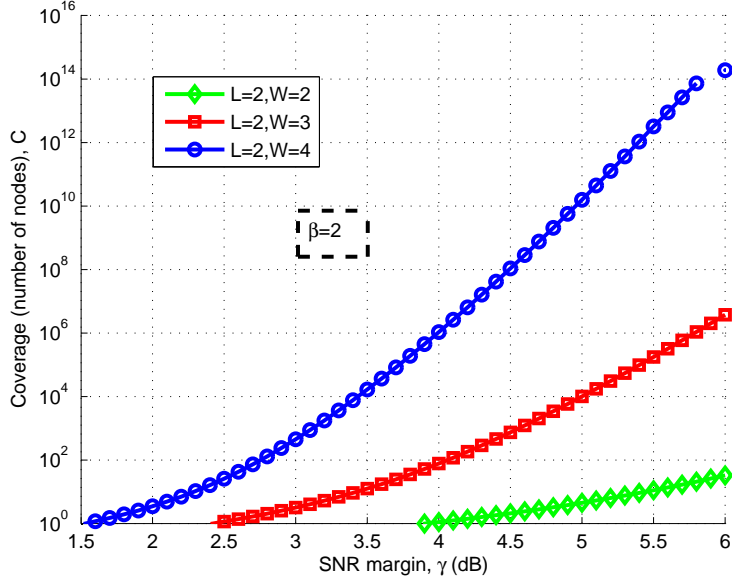


Figure 3.6: SNR margin vs. maximum coverage for various values of M .

nodes, then the information is transmitted towards the far away nodes with lower delay and at high SNR margin. Whereas, if we increase the number of nodes along the width and keep L constant then with the increase in W , diversity increases and information transverses towards its destination with higher delay but at a lower SNR margin. This shows that there is a tradeoff between delay and required SNR margin. Hence, the selection of an optimal STBC and node geometry mainly depends upon the type of application or scenario in which we want to operate, i.e., if the application is more energy-constraint then we select the one that requires lower SNR margin, e.g. half rate STBC with $L = 2$ and $W = 4$, otherwise, for delay sensitive applications, linear or $2D$ geometry having larger L should be used.

In the end, we make a comparison between two topologies discussed before, the distributed and co-located groups topology. The eigenvalues for

Table 3.1: Comparison for optimal STBC and node geometry

M	L	W	$STBC$	Coverage		P	T_d	R	γ (dB)
				\mathcal{C}	ℓ		$P \times \ell$		
4	4	1	3/4 rate	24	6	4	24P	3sym/24P	11.27
4	2	2	3/4 rate	24	12	4	48P	3sym/48P	5.85
6	6	1	3/5 rate	24	4	30	120P	18sym/120P	12.19
6	3	2	3/5 rate	24	8	30	240P	18sym/240P	6.50
6	2	3	3/5 rate	24	12	30	360P	18sym/360P	3.67
8	8	1	1/2 rate	24	3	8	24P	4sym/24P	13.04
8	4	2	1/2 rate	24	6	8	48P	4sym/48P	7.26
8	2	4	1/2 rate	24	12	8	96P	4sym/96P	2.45

distributed and co-located groups topology gives the one-hop success probability and are denoted as ρ_{dis} and ρ_{col} , respectively. In Fig. 3.7, the difference between the two success probabilities, $\rho_{dis} - \rho_{col}$ is plotted vs. the SNR margins for path loss exponent of 2, and that results in a Gaussian-shaped curve. These curves are generated for three different topologies keeping M equal to 6. Fig. 3.7 shows that the maximum difference increases if we arrange more nodes along vertical direction, i.e., larger W in distributed case. These positive difference curve shows that co-located case performs better than distributed one at lower SNR margins. Although, the plots show that the co-located topology gives better success probability than distributed one, however, in some sensing scenarios co-located geometry does not provide accurate or updated information about the points that are spatially distributed. Hence, for these scenarios the nodes need to be arranged in a distributed manner.

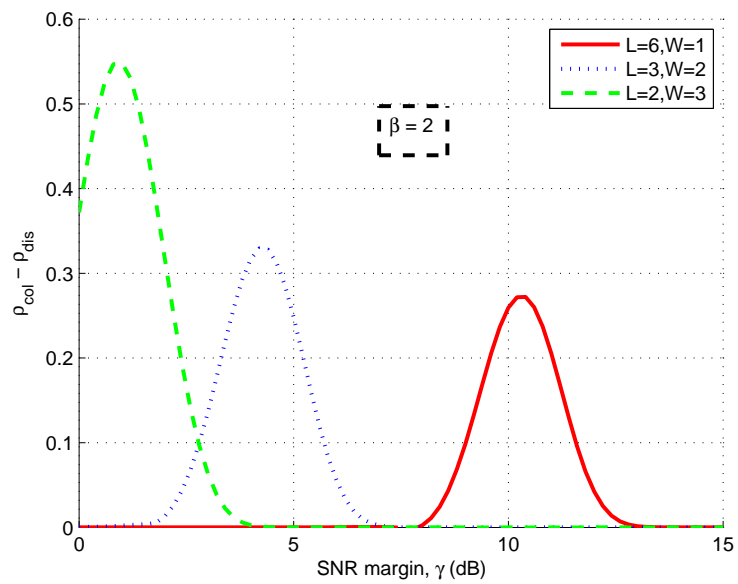


Figure 3.7: One-hop success probability differences between co-located and distributed topologies.

Chapter 4

Near-Orthogonal Space-Time Block Codes

4.1 Introduction

In this chapter, we will discuss the design of near-orthogonal randomized space-time block codes (STBCs) for strip-shaped cooperative multi-hop network having random node geometry in context with the directional statistical concepts. Channel and noise assumptions are same as considered in chapter 3 with transmit and receive times synchronization between DF nodes and receiving nodes, respectively.

4.2 Network Description

Consider an extended strip-shaped cooperative multi-hop network that grows in horizontal direction for a fixed number of nodes, N , placed randomly as shown in Fig. 4.1. Each level forms a bounded $W \times W$ square region of area

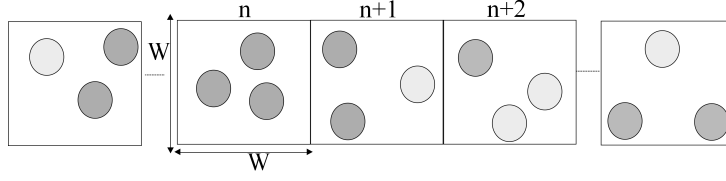


Figure 4.1: Fixed boundary strip network layout with $N = 3$.

\mathcal{A} . In each set of compact area $\mathcal{A} \in \mathbb{R}^2$, N nodes are uniformly distributed using a binomial point process, ϕ , such that $\phi(\mathcal{A}) = N$. These compact set of areas or levels separated through fix boundaries that occurs at regular intervals form a multi-hop strip CN. In this type of network, the nodes that decode the message received from previous $(n - 1)^{th}$ level, relay it to the next $(n)^{th}$ level nodes. The nodes that successfully decode the message become a part of DF set. For our case, DF nodes are represented as filled circles in Fig. 3.1. These nodes decode the message block after comparing the post-detection received signal-to-noise ratio (SNR), from the previous level, with a predefined threshold, τ .

Let a message block $\mathbf{s} = [s_1 \ s_2 \ \dots \ s_b]^T$ needs to be transmitted cooperatively to a far away destination node, where $[\cdot]^T$ denotes the transpose operation and b is the total number of symbols that makes a message block. Each DF node maps the symbol block to an OSTBC, $\mathcal{G}(\mathbf{s})$, so that information can be transmitted in an orthogonal manner towards the next hop of nodes, i.e.,

$$\mathbf{s} \rightarrow \mathcal{G}(\mathbf{s}),$$

where $\mathcal{G}(\mathbf{s}) \in \mathbb{C}^{P \times L}$ is the underlying complex OSTBC matrix having P rows and L columns. The rows represent the time slots a block of symbols will take in transmission from one hop to the next and L is the number of an-

tennas (nodes in our case) in the underlying OSTBC. A potential problem in fully opportunistic CN is that the number of DF nodes in each hop or level is random. Hence, in order to have orthogonal transmission with the deterministic OSTBC for a fully ad-hoc CN, a random independent column vector \mathbf{r}_k of $L \times 1$ at each k^{th} DF node of a specific level is generated as in [31]. These independent random vectors from each of the M DF nodes combine to form a random matrix, \mathcal{R} , of dimension $L \times M$. Each \mathbf{r}_k is being multiplied with underlying OSTBC matrix thus transmitting a linear combination of the symbols in each time slot P . On the other hand, $\mathbf{x}_i = \mathcal{G}(\mathbf{s})\mathcal{R}$ is the random code transmitted from each node, thus

$$\mathbf{s} \rightarrow \mathcal{G}(\mathbf{s}) \rightarrow \mathcal{R}$$

The received signal in P time slots at the k^{th} node of $(n+1)^{th}$ hop can be written as

$$\mathbf{y}_{(n+1)}^{(k)} = Pt\mathcal{G}(\mathbf{s})\mathcal{R}\mathbf{h}^{(k)} + \mathbf{z}, \quad (4.1)$$

where $\mathbf{y}_{(n+1)}^{(k)} \in \mathbb{C}^{P \times 1}$, i.e., $\mathbf{y}_{(n+1)}^{(k)} = [y_1^{(k)} \ y_2^{(k)} \ \dots \ y_P^{(k)}]^T$ is the received signal vector at the k^{th} node of the $(n+1)^{th}$ hop and Pt is the transmitted power, which is assumed equal for all the nodes. The matrix $\mathcal{G}(\mathbf{s}) \in \mathbb{C}^{P \times L}$ is the complex randomized OSTBC whereas, the matrix $\mathcal{R}(\mathbf{s}) = [\mathbf{r}_1 \ \mathbf{r}_2 \ \dots \ \mathbf{r}_M]$ is the randomization matrix. The generation of each $L \times 1$ random vector, \mathbf{r}_k , is explained briefly in the next section. The vector $\mathbf{h}^{(k)} \in \mathbb{C}^{M \times 1}$, i.e., $\mathbf{h}^{(k)} = [h_1^{(k)} \ h_2^{(k)} \ \dots \ h_M^{(k)}]^T$ is the channel vector and the subscript of individual elements denotes the transmitting node from the previous level. The vector, \mathbf{z} , is the complex Gaussian noise vector.

Each $h_j^{(k)}$ from the channel vector represents the fading channel from the j^{th} relay node of the $(n)^{th}$ hop to the k^{th} receiving node of the $(n+1)^{th}$ hop.

The channels between j^{th} transmitting node from the previous level to one of the k^{th} node of next level are stacked to form a vector and this vector is represented in (4.1) as $\mathbf{h}^{(k)}$. Each of these channel gains between a node pair also takes into account the path loss between them. Therefore, we define $h_j^{(k)}$ as, $h_j^{(k)} = \frac{\alpha_{jk}}{d_{jk}^\beta}$, here α_{jk} is the complex Gaussian random variable with zero mean and unit variance, d_{jk} is the random variable for Euclidean distance between the two nodes in our case, and β is the path loss exponent that can be in range of 2-4. The channel is assumed static during the transmission of one block. Therefore, $h_j^{(k)}$ remains constant for the transition of a message block.

As described in [31], there are two interpretations of this randomization technique. We have used the one in which $\mathcal{R}\mathbf{h}^{(k)}$, is considered as a whole, instead of, $\mathcal{G}(\mathbf{s})\mathcal{R}$, in order to simplify decoding procedure at the receiver. This case can be viewed as the deterministic OSTBC, $\mathcal{G}(\mathbf{s})$, transmitted over a random effective channel $\tilde{\mathbf{h}}^{(k)}$. In order to perform coherent decoding, the receiver estimates effective channel coefficients $\tilde{\mathbf{h}}^{(k)}$ instead of estimating $\mathbf{h}^{(k)}$ and \mathcal{R} separately. For that, training sequence at the transmitting nodes has to undergo same randomization procedure.

4.3 Near- Orthogonal Random Matrix

To have orthogonal transmission through the DF nodes, a random vector needs to be generated at each of these nodes. The generation of full-orthogonal random vector at each node without the exchange data is impossible. This implies that the nodes should cooperate in some manner so that orthogonality of relaying information can be preserved. But for our case

it has been assumed that the network is fully opportunistic and the nodes cannot exchange any information. Therefore, we come up with a design of near-orthogonal STBC for cooperative multi-hop opportunistic networks. For this purpose near-orthogonal random vectors need to be generated at the DF nodes so that information can be retrieved at the k^{th} receiving node with a higher success probability.

Many designs have been proposed to generate near-orthogonal independent random vectors. The one that gives the best results and has been used in different applications is a random rotation of random unit vector on the surface of unit hyper sphere \mathcal{S}^{L-1} . This random rotation can be accomplished by multiplying a random vector with special orthogonal (SO) matrices [36] in a series in order to increase the probability of generating, M , ϵ -orthogonal vectors at the DF nodes. Where ϵ should be at least $\pi/3$, i.e., $\pi/3 \leq \epsilon \leq \pi/2$. The generalized form of random vector after application of $SO(L)$ group matrices is, $\mathbf{r}_k = [e^{j\theta_k[0]} \quad e^{j\theta_k[1]} \quad \dots \quad e^{j\theta_k[L]}]^T$, where $\theta_k[m] \sim U(0, 2\pi)$, i.e., uniform distribution in interval $(0, 2\pi)$. In directional statistics, the same concept is addressed as generating random points uniformly on the surface of unit complex/real hyper sphere [32]. The proof of near-orthogonality of these random vectors is given in [37] and it states that as the dimensions L increases for the unit vectors formed from the points generated randomly on sphere, the angles between these random vectors get concentrated around $\pi/2$.

Let us assume that $\|\mathbf{r}_k\|$ is the point generated from the origin as a result of uniform distribution on the surface of unit hyper sphere S^{L-1} where, each \mathbf{r}_k is $L \times 1$ vector whose elements are independent zero-mean and unit-

variance independent complex/real Gaussian . For uniform distribution of point on the hyper sphere each \mathbf{r}_k is normalized, i.e., $\|\mathbf{r}_k\|=1$. Each L-variate random vector $\|\mathbf{r}_k\|$ follows the L-variate Von Mises-Fisher distribution [32]. Whereas, for $L \leq M$, the near-orthogonal matrix \mathcal{R} follows the Von Mises-Fisher matrix distribution or the matrix Langevin distribution and its probability density function (PDF) as given in [38] is

$$\mathbf{P}_{ML}(\mathcal{R}) = \text{etr}(\mathbf{F}'\mathcal{R}) / {}_0\mathbf{F}_1\left(\frac{1}{2}M; \frac{1}{4}\mathbf{F}'\mathbf{F}\right). \quad (4.2)$$

where \mathbf{R} is the random $L \times N$ matrix on Stiefel manifold for $L \leq N$, $\text{etr}(\mathbf{F}) = \exp(\text{tr}\mathbf{F})$ and ${}_p\mathbf{F}_q$ is the hypergeometric function with matrix argument.

4.4 Transmission Modeling

As stated earlier in section II, that random near-orthogonal matrix \mathcal{R} will be combined with channel vector $\mathbf{h}^{(k)}$ to form effective channel vector $\tilde{\mathbf{h}}^{(k)}$. According to [31] performance degradation results in symbol error thus, increasing the symbol error probability, P_e . As long as the underlying OSTBC matrix \mathcal{G} is full rank, i.e., $\text{rank}(\mathcal{G})=L$, it will have no effect on the outage probability. Error matrix can be replaced with the outage which occurs as a result of deep fade event [31].

Let $\left\{\|\mathcal{R}\mathbf{h}^{(k)}\|^2 \leq \tau\right\}$ be the deep fade event that results in outage. Now the probability of not being a deep fade event or the probability of correctly decoding a message block is the success probability $\mathcal{P}_{\text{success}}^{(k)}$ at the k^{th} node of $(n+1)^{\text{th}}$ can be written as

$$\mathcal{P}_{\text{success}}^{(k)}(SNR) = Pr\left\{\|\mathcal{R}\mathbf{h}^{(k)}\|^2 \geq \tau\right\}, \quad (4.3)$$

where $\tau = (SNR)^{-1}$ is a predefined decoding threshold or the required SNR margin. \mathcal{R} in the above expression (4.3) can equivalently be expressed as $\mathcal{R}\mathcal{R}^H$ for eigenvalue decomposition as $\mathbf{U}^H\mathbf{S}\mathbf{U}$, where \mathbf{U} is random matrix and $[\cdot]^H$ denotes the Hermitian operator on a matrix. $\mathbf{S}=\text{diag}(\sigma_1^2, \sigma_2^2, \dots, \sigma_\eta^2)$ are the ordered eigenvalues in descending order of $\mathcal{R}\mathcal{R}^H$ Wishart matrix and $\eta \cong \min\{M, L\}$ denotes the minimum of M and L .

As the nonzero singular values of a complex matrix \mathcal{R} are the square roots of nonzero eigenvalues of $\mathcal{R}\mathcal{R}^H$, i.e.,

$$\sigma_j(\mathcal{R}) = \sqrt{\lambda_j(\mathcal{R}\mathcal{R}^H)}, \quad (4.4)$$

therefore, (4.3) can now be written as

$$\mathcal{P}_{\text{success}}^{(k)}(SNR) = Pr \left\{ \sum_{j=1}^{\eta} \sigma_j^2 |h_j^{(k)}|^2 \geq \tau \right\}. \quad (4.5)$$

Since the distribution for the singular values of matrix Von Mises-Fisher distribution does not exist, therefore, the closed form expression for a success probability at a single receiving node is prohibited.

4.4.1 Markov Chain Modeling of Random Strip OLA Network

The transmissions that propagate from one level to the next follows a Markov chain model as the state of the system at $(n)^{th}$ instant depends upon the previous state. A binary random variable, $\mathbb{I}_j(n)$, represents the state of the j^{th} node of the $(n)^{th}$ level as

$$\mathbb{I}_j(n) = \begin{cases} 0 & \text{node } j \text{ does not decode} \\ 1 & \text{node } j \text{ decodes} \end{cases}, \quad (4.6)$$

For deterministic node geometry, an N -tuple of this binary random variable (RV), i.e., $[\mathbb{I}_1(n) \ \mathbb{I}_2(n) \ \cdots \ \mathbb{I}_N(n)]^T$ represents the overall state of the system at an instant n , as described in Ch.3. But for the network model considered here the inter-nodal distance between the individual nodes of two adjacent levels is no more distinct and fixed. Therefore, for a random node geometry the inter-nodal distance comes out to be random thereby making it difficult to maintain the state of a level in the N tuple form. We, therefore, consider that if any one of the node in a level is in a success then that level will be in state $\mathbf{1}$, which means that the state of the system $\mathcal{B}(n)$ is equal to the number of DF nodes at $(n)^{th}$ instant, i.e.,

$$\mathcal{B}(n) = \sum_{j=1}^N \mathbb{I}_j(n). \quad (4.7)$$

\mathcal{B} therefore forms a finite state Markov chain as the state of $(n)^{th}$ level depends upon the state of previous $(n-1)^{th}$ level. The Markov chain \mathcal{B} can be completely defined by the union of two sets, the transient state space X and the absorbing state $\{0\}$ where,

$$X = \left\{ \begin{array}{ll} 1 & \text{One node is in success} \\ 2 & \text{Two nodes are in success} \\ \cdot & \cdot \\ \cdot & \cdot \\ \cdot & \cdot \\ N & \text{All N nodes are in success} \end{array} \right. \quad (4.8)$$

The set $\{0\}$ is the absorbing state and it refers to state when all the nodes fails to decode the message thus terminating the message propagation. Hence, the sub-stochastic transition probability matrix \mathbf{P} with active states

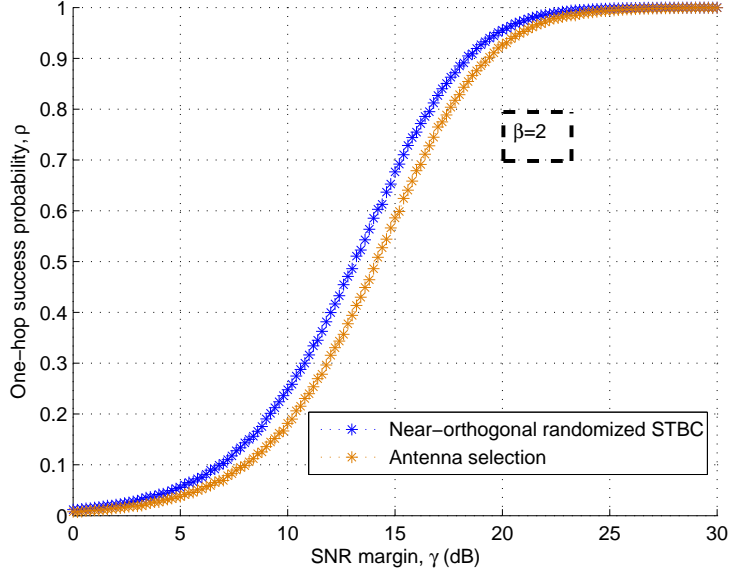


Figure 4.2: One-hop success probability comparison between Nearly-orthogonal randomized STBC and antenna selection technique for $L = N = 2$.

transition probabilities for a given Markov chain will have dimensions, $N \times N$, removing the transitions to and from the absorbing state. The Perron-Frobenius theorem [34] is then invoked on \mathbf{P} to get maximum eigenvalue ρ , which is the one-hop success probability. Where, $0 < \rho < 1$ implies that the square matrix \mathbf{P} is not right stochastic as the sum of row probabilities does not equal to 1.

4.5 Results and Analysis

In this section, we present various results pertaining to the performance of cooperative multi-hop strip-shaped network with random nodes geometry,

employing near-orthogonal random STBC. Comparisons and analysis have been made by considering different number of nodes per hop, N , for different or same underlying STBC columns, L . We obtain the results for the one-hop success probability and coverage through Monte Carlo methods for 30,000 iterations of a symbol block and for $W = 6$. In the following, the channel coefficients are considered independent and identically distributed (i.i.d) having a complex Gaussian distribution, i.e., $h_j^{(k)} \sim \mathcal{N}_c(0, 1)$.

In Fig. 4.2, the performance of near-orthogonal random STBC is shown as compared to the antenna selection random STBC technique. In antenna selection scheme [31], each DF node randomly selects an STBC column by randomly generating a unit canonical vector such that, $\mathbf{r}_k \in Q = \{e_k, k = 1, \dots, L\}$. The comparison is made on the basis of one-hop success probability, ρ , for different values of SNR margin, γ , where γ is the normalized SNR and it is defined as, $\gamma = \frac{P_r}{\sigma^2 \tau}$. The path loss exponent, $\beta=2$ is considered for all the results. To determine the one-hop success probability, the entries of transition probability matrix \mathbf{P} are computed using expressions (4.5)-(4.8) for 30,000 iterations of a message block for a single value of γ . $N = 2$ and $L = 2$ is considered for the result shown in Fig. 4.2. Here $\mathcal{G}(\mathbf{s})$ is the Alamouti code, i.e.,

$$\mathcal{G}(\mathbf{s}) = \begin{bmatrix} s_1 & s_2 \\ -s_2^* & s_1^* \end{bmatrix},$$

where $\mathbf{s} = \begin{bmatrix} s_1 & s_2 \end{bmatrix}$ is the transmitted symbols block. The trend in Fig. 4.2 shows that the one-hop success probability increases with the increase in γ , where increase in γ results in a decreased τ hence, allowing more nodes to

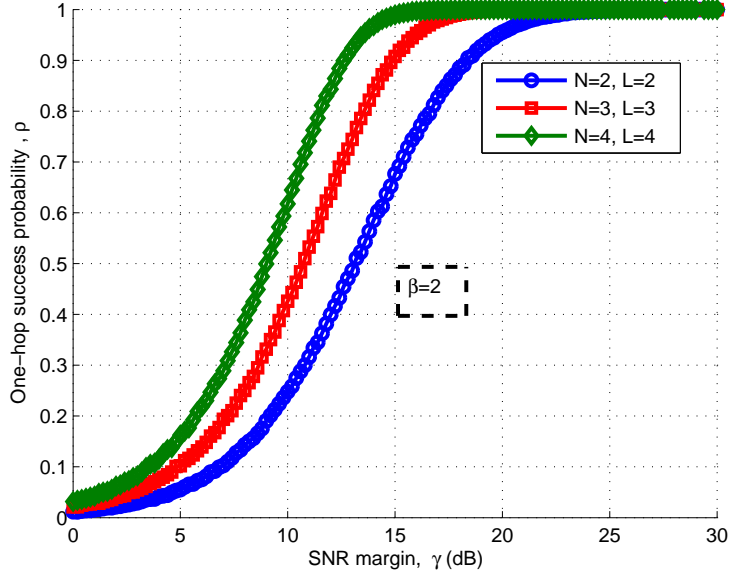


Figure 4.3: One-hop success probability for cooperative multi-hop strip-shaped networks for $L = N$.

decode. Besides that Fig. 4.2 also depicts that the near-orthogonal random STBC has a better performance in terms of one-hop success probability as compared to the antenna selection scheme for the network model shown in Fig. 4.1. As for 90% success probability, antenna selection requires a high SNR margin than the near-orthogonal random STBC technique.

Fig. 4.3 demonstrates the behavior of one-hop success probability, ρ , for different values of N and corresponding values of L . This implies that the underlying STBC code is selected on the basis of node density in each hop, i.e., $\phi(\mathcal{A}) = N$. The details regarding the rate of STBCs are given in [11, 12, 13, 14]. The trend of ρ is same as in Fig. 4.2 but increasing N and L requires higher γ to achieve the same one-hop success probability.

Fig. 4.4 represents one-hop success probability trend, ρ , for different

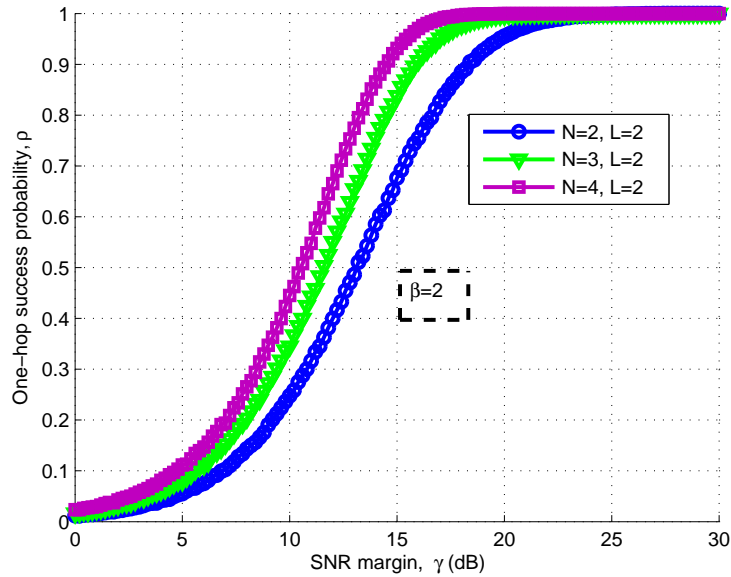


Figure 4.4: One-hop success probability comparison of near-orthogonal randomized STBC for $L = 2$.

values of nodes per hop, N , keeping L constant. As previously Alamouti code is utilized. Fig. 4.4 shows that increasing N improves the system performance as at the larger values of N lower value of γ is required for same value of ρ . The reason behind this is that sometimes same information is being sent out through all the N independent channels thereby increasing the overall spatial diversity.

In Fig. 4.5 and Fig. 4.6, network performance is analyzed by evaluating coverage in terms of maximum number of hops traversed by a message block. In Fig. 4.5, coverage, C , is being plotted against γ for different values of N and L as considered for Fig. 4.3. Whereas, Fig. 4.6 shows coverage for a constant L and increasing values of N . Multiple block of symbols are being transmitted for coverage analysis from the first hop of the OLA network to

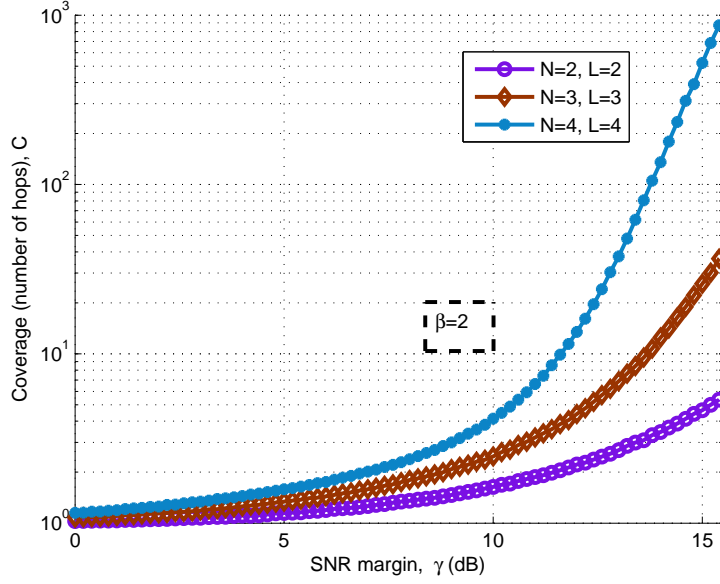


Figure 4.5: Coverage vs. SNR margin for near-orthogonal randomized STBC, $L = N$.

the next until the absorbing state $\{0\}$ is reached. Let ℓ be the hop/instant at which absorbing state occurs then, $C = \ell - 1$ are the number of hops that are coverage. The general trend in both the figures show that the coverage value increases non-linearly with the increase in γ as, the one-hop success probability increases.

In the end overall comparison of multi-hop strip-shaped cooperative network is being summarized in Table 4.1, where P is the number of time slots consumed to transmit a message block from one hop to the next, T_d is the overall delay up to C^{th} hop, and R is the rate of the transmissions through strip-shaped OLA network for different node densities and underlying OSTBC columns. The table figures out the effect of node density, N , and OSTBC on latency, T_d , rate, R , and required SNR margin, γ for a fixed

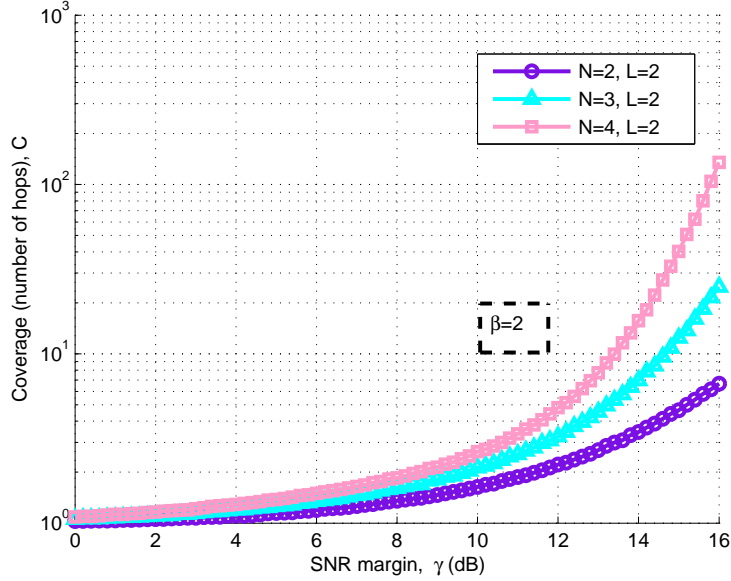


Figure 4.6: Coverage comparison for $L = 2$.

coverage range in terms of number of hops, i.e., $C = 6$. Specifications of OSTBCs are provided in Ch. 3. Considering a case in which $N = 4$ and $L = 4$, an underlying OSTBC of rate $3/4$ is used, that transmits a block of 3 symbols in 4 time slots from one hop to the next. Therefore, it will take 24 time slots to transmit a block of 3 symbols to the 6th hop at a required SNR margin of 10.8 dB. From Table 4.1, it can be deduced that if an underlying OSTBC having L orthogonal columns is selected according to the per hop node density, N , such that $L = N$ then, more information symbols can be transmitted towards the far away nodes with almost same rate and at lower SNR margin. Whereas, for constant L and increasing values of N same number of hops can be traversed with same rate and lower SNR margin, γ , which is still greater than the one in which L is increased correspondingly. Hence, optimal near-orthogonal randomized STBC for strip-shaped OLA network

Table 4.1: Comparison for the optimal combination of L and N for $W = 6$

N	L	$STBC$	Coverage	P	T_d	R	γ (dB)
			\mathcal{C}		$P \times \mathcal{C}$	b/T_d	
2	2	full rate	6	2	12P	2sym/12P	15.7
3	2	full rate	6	2	12P	2sym/12P	13.7
3	3	3/4 rate	6	4	24P	3sym/24P	12.5
4	2	full rate	6	2	12P	2sym/12P	12.5
4	4	3/4 rate	6	4	24P	3sym/24P	10.8

requires L to be equal to N .

Chapter 5

Conclusion and Future Work

5.1 Conclusion

In this thesis, we have proposed a way:

- To construct orthogonal channels by using STBCs for $2D$ opportunistic large array sensor networks. Deterministic STBCs are made random with the help of indicator or state vector, which are then used by the random opportunistic nodes at each level. Markov chain and Perron-Frobenius eigenvalue decomposition are used to completely model the network state and the transmission strategy. The performance of the network in terms of success probability, maximum coverage, and transmission rate is then analyzed at different SNR margins. The success probability comparison between distributed and co-located group node geometries has been made. The results show that the choice of optimal node geometry and underlying OSTBC is purely application dependent.
- To construct near-orthogonal channels by preserving the opportunistic

nature of OLA network. Directional statistical techniques are utilized for the generation of random independent near-orthogonal column vectors at the DF nodes. The PDF expressions for near-orthogonal random independent column vectors and randomization matrix are introduced. The outage event is considered to occur when the channel undergoes a deep fade. Transmissions are modeled using Markov chain that eventually end up in an absorbing state thereby making it a quasi-stationary Markov chain. Perron-Frobenius eigenvalue decomposition are used to completely model the network state. Techniques that were proposed previously are compared on the basis of one-hop success probability. Coverage analysis is being presented while taking in account the overall rate and latency, the system will undergo.

5.2 Future Work

Some of the possible future directions of this work are:

- To extend the design proposed in chapter 4, by exploring more advance concepts of directional statistics in the light of quaternions and Clifford variables that may further improve the network performance. As, the design of STBCs for fixed number of antennas using quaternions and Clifford variables is also a hot topic in research [39, 40].
- To analyze the behavior of these proposed randomized STBC designs for different fading environments with and without shadowing.
- To design randomized STBC by considering random number of nodes in each level.

- To remove the fixed boundary constraint which will result in in-homogeneous Markov chain for transmission modeling of a pure OLA network.

Bibliography

- [1] M. Jankiraman, "Space-Time Codes and MIMO Systems," *Artech House Universal Personal Communications Series*, Jul. 2004.
- [2] S. A. Hassan, Y.G. Li, P.S.S. Wang, and M. Green, "A full rate dual relay cooperative system for wireless communications," *IEEE Journal on Communications and Networks (JCN)*, vol. 12, no. 5, pp. 442-448, Oct. 2010.
- [3] M. Bacha and S. A. Hassan, "Performance analysis of cooperative linear networks subject to composite shadowing fading," *IEEE Trans. Wireless Commun.*, vol. 12, no. 11, pp. 5850-5858, Nov. 2013.
- [4] S. Yang, J. C. Belfiore, "Towards the optimal amplify-and-forward cooperative diversity scheme," *IEEE Transactions on Info. Theory*, vol. 53, no. 9, pp. 3114-3126, Sept. 2007.
- [5] A. Nosratinia, T. E. Hunter, A. Hedayat, "Cooperative communication in wireless networks," *IEEE Communications Magazine*, vol. 42, no. 10, pp. 74-80, Oct. 2004.
- [6] A. Scaglione and Y. Hong, "Opportunistic large arrays: cooperative transmission in wireless multi-hop ad hoc networks to reach far dis-

- tances,” *IEEE Trans. Signal Process.*, vol. 51, no. 8, pp. 2082-2092, Aug. 2003.
- [7] S. A. Hassan and M. A. Ingram, “Analysis of an opportunistic large array line network with Bernoulli node deployment,” *IET Communications*, vol. 8, no. 1, pp. 19-26, Jan. 2014.
- [8] M. Bacha and S. A. Hassan, “Distributed versus Cluster-Based Cooperative Linear Networks: A Range Extension Study in Suzuki Fading Environments,” *In Proc. IEEE Personal Indoor and Mobile Radio Communications (PIMRC)*, 2013, London, UK.
- [9] R. I. Ansari and S. A. Hassan, “Opportunistic large array with limited participation: An energy-efficient cooperative multi-hop network,” *IEEE International Conference on Computing, Networking and Communications (ICNC)*, pp. 831-835, Feb. 2014.
- [10] S. M. Alamouti, “A simple transmitter diversity scheme for wireless communications,” *IEEE J. Sel. Areas Commun.*, vol. 16, no. 10, pp.1451-1458, Oct. 1998.
- [11] Weifeng Su and Xiang-Gen Xia, “Two generalized complex orthogonal space-time block codes of rates $7/11$ and $3/5$ for 5 and 6 transmit antennas,” *IEEE Trans. Inf. Theory*, vol. 49, no. 1, pp. 313-316, Jan. 2003.
- [12] Santumon.S.D and B.R. Sujatha, “Space-time block coding (STBC) for wireless networks,” *International Journal of Distributed and Parallel Systems (IJDPS)*, vol. 3, no. 4, pp. 183-195, Jul. 2012.

- [13] M. Rupp and C. F. Mecklenbrauker, "Spacetime block coding for wireless communications: performance results," *IEEE, Wireless Personal Multimedia Communications . The 5th International Symposium on* , vol. 1, pp. 115-119, Oct. 2002.
- [14] V. Tarokh, H. Jafarkhani, and A. R. Calderbank, "On extended Alamouti Schemes for space-time coding," *IEEE Journal on Selected Areas in Commun.*, vol. 17, no. 3, pp. 451-460, Mar. 1999.
- [15] M. C. Valenti and D. Reynolds, "Cooperative cellular wireless networks ," *Cambridge University Press*, 2011.
- [16] V. C. Gungor, D. Sahin, T. Kocak, S. Ergt, C. Buccella, C. Cecati, and G. P.Hancke, "Smart grid technologies: communication technologies and standards," *Industrial Informatics, IEEE Transactions*, vol. 7, no. 4, pp. 529-539, Sep. 2011.
- [17] G. J. Foschini and M. J. Gans, "On limits of wireless communications in a fading environment when using multiple antennas," *Wireless Pers. Commun.*, vol. 6, no. 3, Mar 1998, pp. 331-335.
- [18] S. Ma, Y. Yang, and H. Sharif , "Distributed MIMO technologies in cooperative wireless networks," *Advances in Cooperative Wireless Networking, IEEE Communication Magazine*, May 2011.
- [19] J. N. Laneman, D. N. C. Tse, and G. W. Wornell, "Cooperative diversity in wireless networks: Efficient protocols and outage behavior," *IEEE Trans. Inf. Theory*, vol. 50, pp. 3062-3080, Dec. 2004.

- [20] M. B. Haroon and S. A. Hassan, "On the Impacts of lognormal-Rice Fading on Multi-Hop Extended Networks," *IEEE International Wireless Communications and Mobile Computing Conference (IWCMC)*, pp. 529-539, Aug. 2014.
- [21] S. A. Hassan and M. A. Ingram, "A quasi-stationary Markov chain model of a cooperative multi-hop linear network," *IEEE Trans. Wireless Commun.*, vol. 10, no. 7, pp. 2306-2315, Jul. 2011.
- [22] S. A. Hassan and M. A. Ingram, "Modeling of a cooperative one-dimensional multi-hop network using quasi-stationary Markov Chains," *IEEE Global Commun. Conf. (Globecom)*, pp. 1-5, Dec. 2010.
- [23] S. A. Hassan and M. A. Ingram, "A stochastic approach in modeling cooperative line networks," *IEEE Wireless Commun. and Networking Conf. (WCNC)*, pp. 1322-1327, Mar. 2011.
- [24] S. A. Hassan and M. A. Ingram, "On the modeling of randomized distributed cooperation for linear multi-hop networks," *IEEE Intl. Conf. Communications (ICC)*, pp. 366-370, Jun. 2012.
- [25] S. A. Hassan, "Performance analysis of cooperative multi-hop strip networks," *Springer Wireless Personal Commun.*, vol. 74, no. 2, pp. 391-400, Jan. 2014.
- [26] Q. Shafi and S. A. Hassan , "Interference analysis in cooperative multi-hop networks subject to multiple flows," *IEEE IFIP Wireless Days (WD)*, Nov. 2014.

- [27] M. Hussain and S. A. Hassan, "Imperfect timing synchronization in multi-hop cooperative networks: statistical modeling and performance analysis," *IEEE IFIP Wireless Days (WD)*, Nov. 2014.
- [28] S. A. Hassan, "Range extension using optimal node deployment in linear multi-hop cooperative networks," *IEEE Radio and Wireless Symposium (RWS)*, vol. 74, no. 2, pp. 364-366, Jan. 2013.
- [29] S. Yiu, R. Schober, and L. Lampe, "Distributed space-time block coding," *IEEE Trans. Commun.*, vol. 54, no. 7, pp. 1195-1206, Jul. 2006.
- [30] B. S. Mergen and A. Scaglione, "Randomized distributed space-time coding for cooperative communication in self-organized networks," *IEEE Proc. Signal Process. Advances in Wireless Commun. (SPAWC)*, 6th workshop, pp. 500-504, Jun. 2005.
- [31] B. S. Mergen and A. Scaglione, "Randomized distributed space-time coding for distributed cooperative communications," *IEEE Trans. Signal Process.*, vol. 55, no. 10, pp. 5003-5017, Oct. 2007.
- [32] A. Banerjee, I. S. Dhillon, J. Ghosh, S. Sra, "Clustering on the unit hypersphere using Von Mises-Fisher distributions," *Journal of Machine Learning Research*, vol. 6, pp. 1345 - 1382, Jan. 2005.
- [33] R. Vaze and R. W. Heath, "Cascaded orthogonal space-time block codes for wireless multi-hop relay networks," *EURASIP Journal on Wireless Commun. and Networking*, Apr. 2013.

- [34] A. Afzal and S. A. Hassan, "Stochastic modeling of cooperative multi-Hop strip networks with fixed hop boundaries," *IEEE Trans. Wireless Commun.*, vol. 13, no. 8, pp. 4146-4155, Aug. 2014.
- [35] S. A. Hassan and M. A. Ingram, "Benefit of co-locating groups of nodes in cooperative line networks," *IEEE Commun. Letters*, vol. 16, no. 2, pp. 234-237, Feb. 2012.
- [36] W. K. Tung and M. Aivazis, "Group Theory in Physics," 1985.
- [37] T. Cai, J. Fan, and T. Jiang, "Distributions of angles in random packing on spheres," *The Journal of Machine Learning Research*, pp. 1837 - 1864, Jan. 2013.
- [38] Y. Chikuse, "Concentrated matrix Langevin distributions," *Journal of Multivariate Analysis*, vo.85 pp. 375 - 394, 2013.
- [39] T. Unger and N. Markin, "Quadratic forms and space-time block codes from generalized quaternion and bi-quaternion algebras," *IEEE Transactions on Information Theory*, vol. 57, no. 9, pp. 6148-6156, Sep. 2011.
- [40] S. Karmakar, B.S.Rajan, "Minimum-decoding-complexity, maximum-rate space-time block codes from Clifford algebras," *IEEE International Symposium on Information Theory*, pp. 788-792, Jul. 2006.